Electronic Supplementary Information

Metal-Organic Gel Coupled Entropy-Driven Circuit for Fluorescence Detection of miR-155

Li Ping Cao, [a] Yao Wang, [a] Yan Bai,[a] Yong Jian Jiang, [a] Chun Mei Li, [a] Yuan Fang Li, [b] Cheng Zhi Huang*[a] and Shu Jun Zhen*[b]

[a] Key Laboratory of Luminescence Analysis and Molecular Sensing (Southwest University), Ministry of Education, College of Pharmaceutical Sciences, Southwest University, Chongqing 400715, P. R. China.

[b] Key Laboratory of Luminescent and Real-Time Analytical System (Southwest University), Chongqing Science and Technology Bureau, College of Chemistry and Chemical Engineering, Southwest University, Chongqing 400715, P. R. China.

*Corresponding author, E-mail address: chengzhi@swu.edu.cn (Cheng Zhi Huang), zsj@swu.edu.cn (Shu Jun Zhen).

Tel: (+86) 23 68254659; Fax: (+86) 23 68367257.

*Corresponding author. Tel: 86-23-68254659; E-mail addresses: chengzhi@swu.edu.cn, zsj@swu.edu.cn

Table S1. Oligonucleotide sequences used in this work

Name	Sequence（5′-3′）
SS	ACCCCTATCACGATTAGCATTAAAGGGCCGTAAGAGAGCT GTAGATTGGATCG
OS	FAM-CCCTTTAATGCTAATCGTGAT
AS	CGATCCAATCTACAGCTCTCTTACGG
fuel	CGATCCAATCTACAGCTCTCTTACGGCCCTTTAATGCTAAT CGTGAT
miR-155	UUAAUGCUAAUCGUGAUAGGGGU
miD-155	TTAATGCTAATCGTGATAGGGGT
Mis-1	UUAAUCCUAAUCGUGAUAGGGGU
Mis-2	UUAAUCCUAAUCGUGAUAGCGGU
Mis-3	UUAAUCCUAAUAGUGAUAGCGGU
Mis-4	UUAAUCCUAAUAGUGUUAGCGGU
miR-21	UAGCUUAUCAGACUGAUGUUGA
let-7a	UGAGGUAGUAGGUUGUAUAGUU

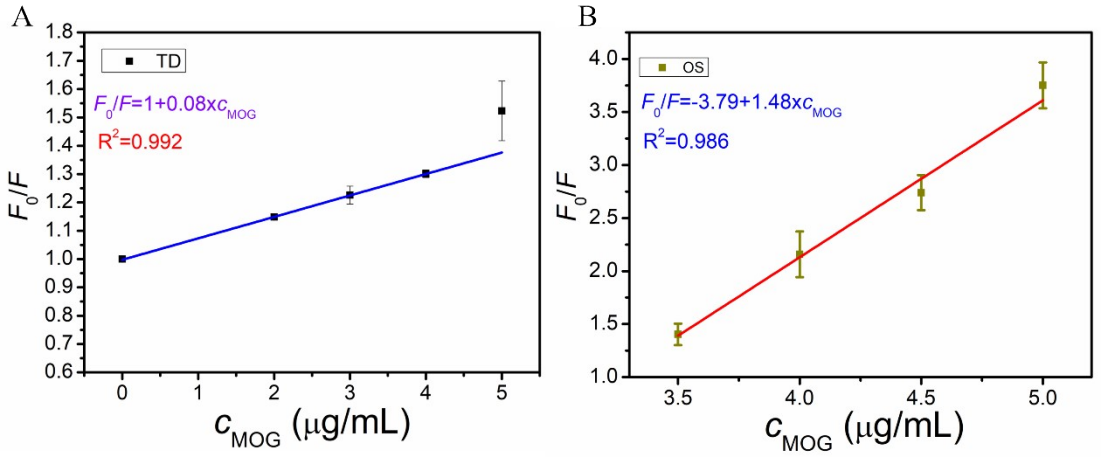

Fig. S1. The quenching constant of TD (A) and OS (B). The concentration of TD and OS were 100 nM and 200 nM, respectively.

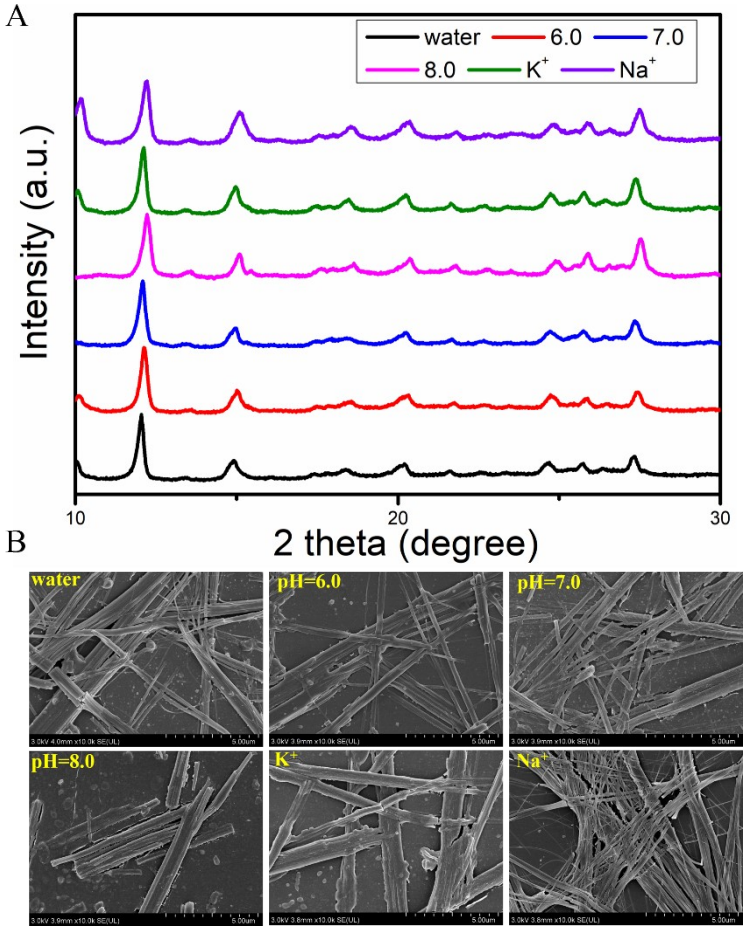

Fig. S2. The examination of Cu-MOG hydrostability. (A) The XRD spectra of Cu-MOG in the aqueous solutions with different pH values and inorganic ions. (B) The SEM images of Cu-MOG in the aqueous solutions with different pH values and inorganic ions.

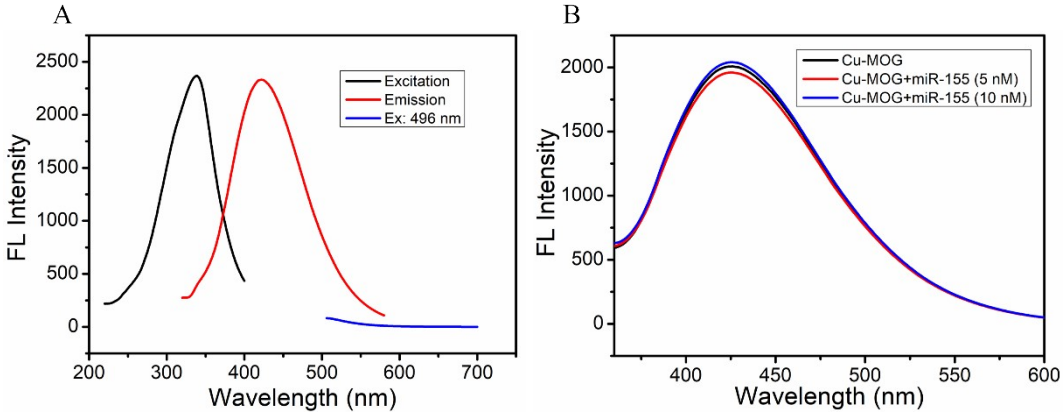

Fig. S3. The fluorescence curve of Cu-MOG. (A) The excitation and emission spectra of Cu-MOG. (B) The fluorescence curve of Cu-MOG in the presence of miR-155 under excitation wavelength of 338 nm.

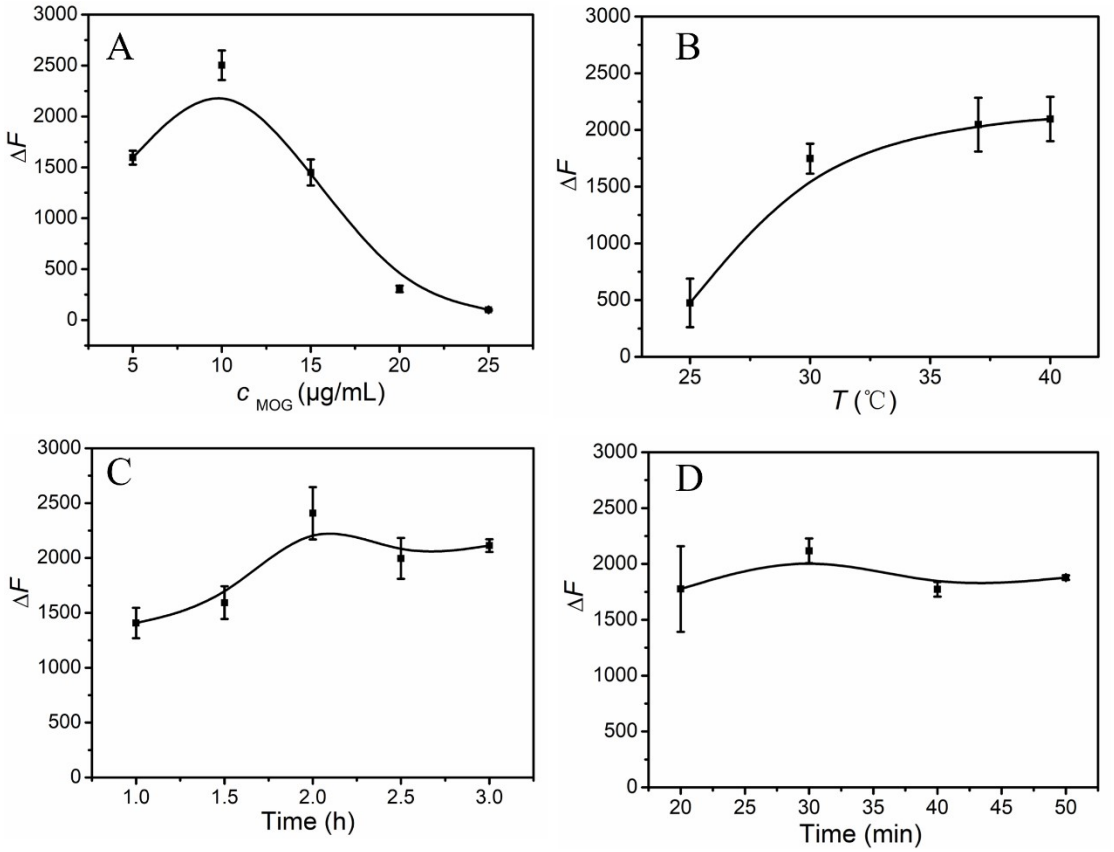

Fig. S4. Optimization of experimental conditions. (A) Concentration optimization of Cu-MOG; (B) EDC reaction temperature optimization. (C) EDC reaction time optimization. (D) Optimization of incubation time of Cu-MOG. The experimental conditions were as follows: the concentrations of TD and fuel were 100 nM, and the concentration of miR-155 was 3 nM. The ribonuclease inhibitor concentration was 25 U/mL.

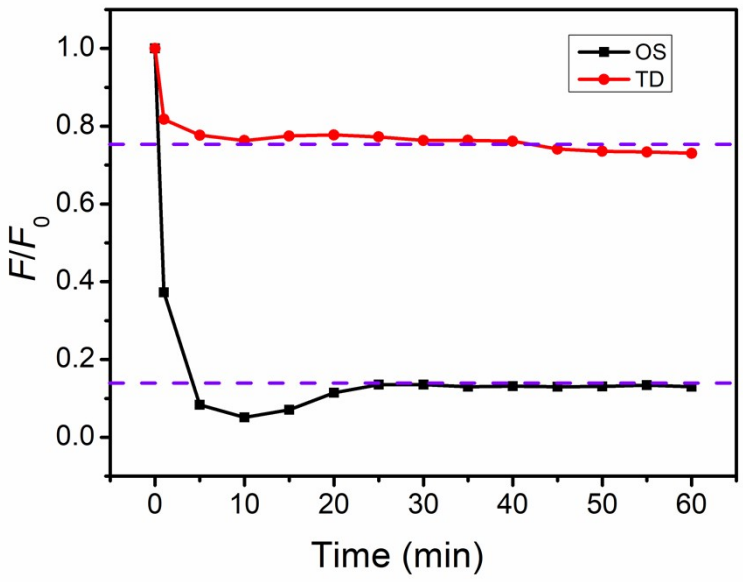

Fig. S5. The adsorption kinetics of OS and TD on Cu-MOG.

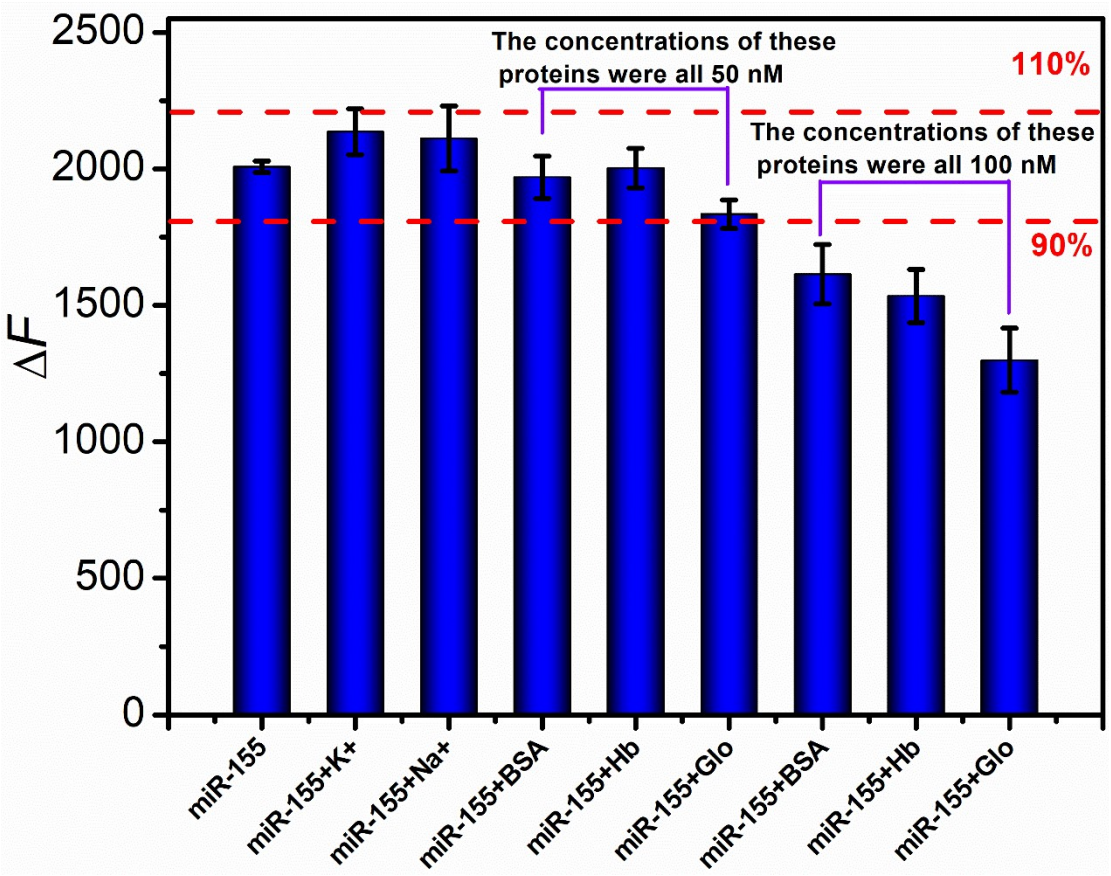

Fig. S6. The anti-interference ability of this method. The concentration of miR-155 was 3 nM, and the concentrations of K^+ and Na^+ were 5 mM and 140 mM, respectively. In addition, the low concentrations of these proteins were all 50 nM and the high concentrations of these proteins were all 100 nM. The red dashed line showed the value of the miR-155 response fluctuating by 10%.

Table S2. Recovery tests of miR-155 detection in 10000-fold diluted human serum samples (*n*=3) [a].

Sample	Added (nM)	Found (nM) Mean[b]±SD[c]	Recovery(%)	RSD (%)
1	1.00	1.06±0.01	106.33±1.25	1.17
2	3.00	3.12±0.10	104.00±3.31	3.18
3	5.00	4.88±0.07	97.67±1.41	1.44

[a] The human serum samples were acquired from the Southwest Hospital, Chongqing, China. [b] The mean of three determinations. [c] SD = standard deviation.

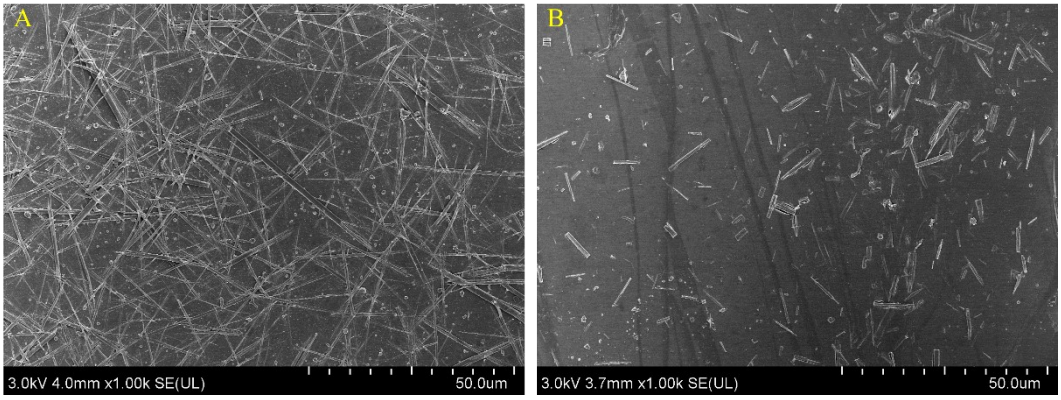

Fig. S7. The SEM images of Cu-MOG before (A) and after (B) sensing.

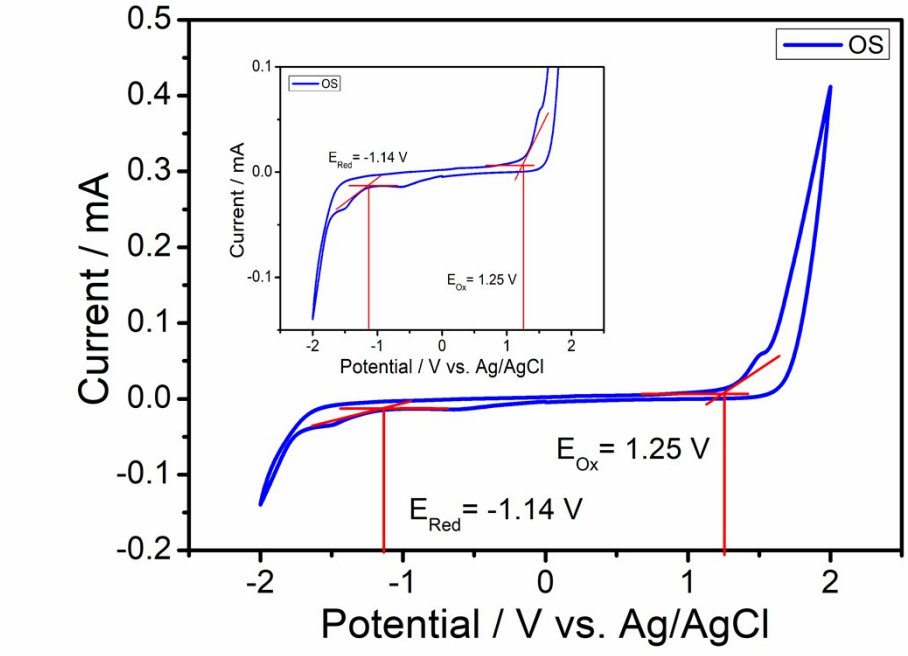

Fig. S8. The cyclic voltammetry curves of OS. Inset: amplification of delineating potential.

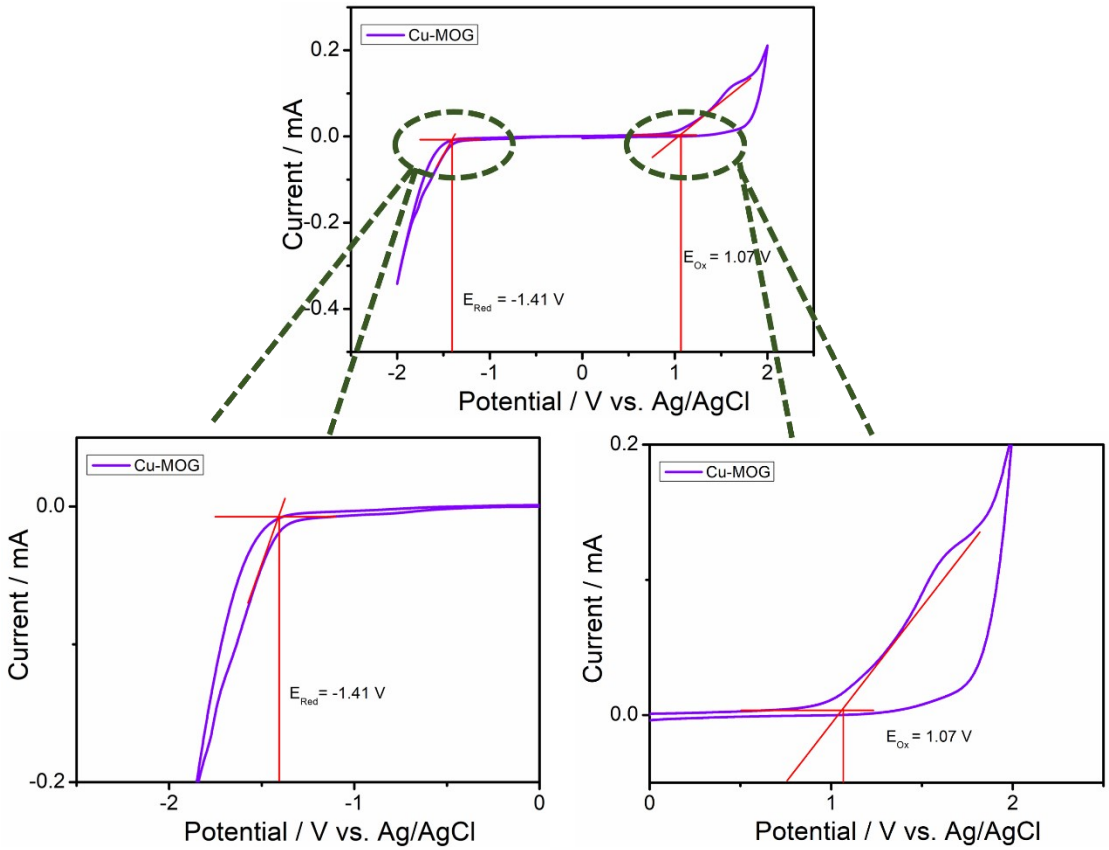

Fig. S9. The cyclic voltammetry curves of Cu-MOG. The figure above showed the whole and the figure below showed the amplification of delineating potential.

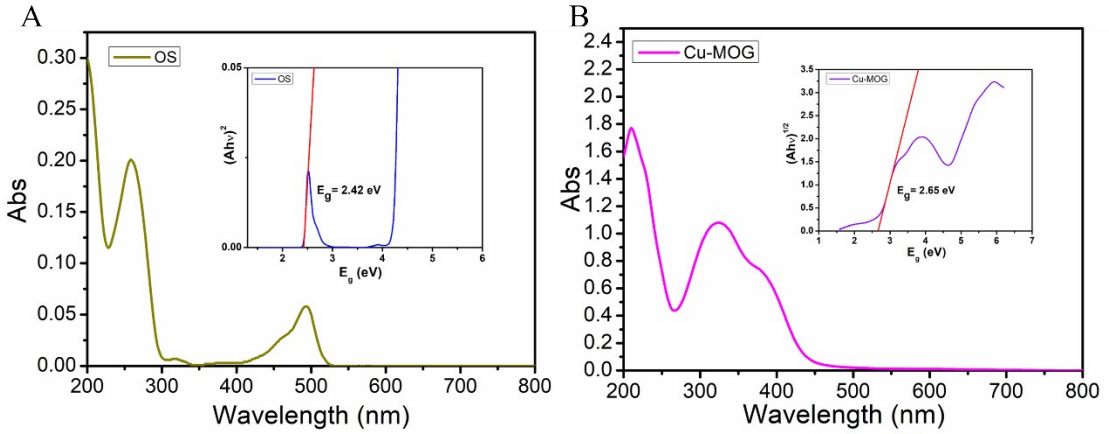

Fig. S10. The absorption of OS (A) and Cu-MOG (B). Inset: Optical bandgap determined from Taut plot $(Ahν)^2$ *vs.* (hν) of indirect semiconductor and $(Ahν)^{1/2}$ *vs.* (hν) of direct semiconductor, where A is absorbance.